Journal of Inflammation Research

Dovepress
Taylor & Francis Group

Open Access Full Text Article

ORIGINAL RESEARCH

# From Gene to Intervention: NLRC4 and WIPI1 Regulate Septic Acute Lung Injury Through Autophagy

Xinyi Yang[1,2,*], Zhijian Sun[1,2,*], Zhuohui Liu[1,2,*], Hui Chen[1,2], Yang Fang[1,2], Wenqiang Tao[1,2], Ning Zhao[1,2], Xiufang Ouyang[1,2], Fen Liu[1,3], Kejian Qian[1]

[1]Department of Critical Care Medicine, the First Affiliated Hospital, Jiangxi Medical College, Nanchang University, Nanchang, 330006, People's Republic of China; [2]Medical Innovation Center, the First Affiliated Hospital, Jiangxi Medical College, Nanchang University, Nanchang, 330006, People's Republic of China; [3]Jiangxi Medical Center for Critical Public Health Events, the First Affiliated Hospital, Jiangxi Medical College, Nanchang University, Nanchang, 330052, People's Republic of China

*These authors contributed equally to this work

Correspondence: Kejian Qian; Fen Liu, Email ndyfy00754@ncu.edu.cn; ndyfy01300@ncu.edu.cn



**Background:** Septic Acute Lung Injury (SALI)-induced severe respiratory dysfunction has been established to significantly increase patient mortality rates and socioeconomic costs. To mitigate cellular damage, autophagy —a conserved biological process in organisms —degrades damaged cellular components, such as proteins and organelles. Although autophagy is crucially involved in the inflammatory response, its precise molecular mechanisms in SALI remain unclear, forming the basis of this study.

**Methods:** Herein, two microarray datasets (GSE33118 and GSE131761) and three single-cell sequencing datasets (SCP43, SCP548, and SCP2156) derived from human samples were used to ascertain the interrelationship between Differentially Expressed Autophagy-Related Genes (DEARGs) and SALI. The relationship between key DEARGs and SALI was validated both in vitro and in vivo using various techniques, including flow cytometry, Immunofluorescence (IF), Quantitative Polymerase Chain Reaction (qPCR), Western Blotting (WB), and small interfering RNA (siRNA).

**Results:** Herein, we found that autophagy activation attenuated SALI, with NLRC4 and WIPI1 as the two key DEARGs involved. Specifically, NLRC4 and WIPI1 downregulation mitigated SALI via autophagy activation. Compared to NLRC4, WIPI1 was more closely associated with noncanonical autophagic flux in SALI. Furthermore, immune infiltration analysis and single-cell data showed a close relationship between NLRC4, WIPI1, and immune cells.

**Conclusion:** Our findings revealed that SALI correlated strongly with autophagy, with the downregulation of the two key DEARGs, NLRC4 and WIPI1, attenuating sepsis lung injury via autophagy regulation, highlighting their therapeutic significance in SALI.

**Keywords:** septic acute lung injury, autophagy, immunity, bioinformatics

## Introduction

Sepsis, a medical condition with a high mortality rate globally,[1] is characterized by the dysregulation of the body's innate immune response to invading pathogens, resulting in multiorgan dysfunction.[2] Septic Acute Lung Injury (SALI) is one of the earliest and most severe complications of sepsis in its later stages,[3] encompassing complex pathological processes involving multiple cellular and molecular interactions.[4,5] Presently, effective strategies to mitigate intrapulmonary inflammation and decelerate the pathological progression of sepsis remain elusive in clinical practice. Furthermore, it is not yet fully understood which autophagy targets are involved in the pathogenesis of SALI. Therefore, this study sought to identify novel therapeutic avenues for SALI, focusing on new targets for pathological regulation.

Autophagy, a lysosome-dependent process that facilitates the degradation of damaged proteins and organelles,[6] is crucially involved in multiple cellular processes, including metabolic homeostasis,[7] cell fate determination, and inflammatory response regulation.[8] We previously demonstrated that autophagy activation attenuates SALI by inhibiting

Received: 6 December 2024
Accepted: 4 March 2025
Published: 12 March 2025

inflammatory vesicle activation.[9] Furthermore, mitochondrial autophagy activation was shown to protect against septic lung injury and inhibit inflammation progression in the lungs.[10] Moreover, blood specimens derived from SALI patients recently exhibited impaired autophagic flux.[11] Despite growing evidence on the role of autophagy in inflammatory processes, its specific molecular mechanisms in SALI remain unclear,[12] forming the basis of this study.

Herein, several methodologies were used to examine the physiological mechanisms underpinning SALI, focusing on key therapeutic targets. Differentially Expressed Autophagy-Related Genes (DEARGs) in sepsis lung injury were identified through bioinformatics analysis. The correlation between DEARGs and immune cell regulation was also explored, with in vitro and in vivo models verifying that two DEARGs —NLRC4 and WIPI1—could serve as key targets for SALI regulation. Therefore, the correlation between autophagy and SALI via NLRC4 and WIPI1 regulation was explored further. Besides elucidating the molecular mechanisms of SALI, this study also identified novel molecular targets for therapeutic protocols.

# Methods

## Data Collection

The GSE33118 dataset[13] from the Gene Expression Omnibus (GEO) database (https://www.ncbi.nlm.nih.gov/geo/),[14] which contains 20 blood samples from patients with pulmonary infection-induced septic shock (collected within 12 h of diagnosis) and 42 blood samples from healthy controls, was used for the primary analysis. The data were annotated using the GPL570 platform (http://www.affymetrix.com/index.affx). They were then subjected to bioinformatics analysis after standardization, annotation, $\log_2$ transformation, and quantile normalization. To ascertain the reliability of the bioinformatics results, the key genes were validated using data from the GSE13176115 dataset.[15] According to the "Measures for Ethical Review of Human Life Science and Medical Research" issued by China on February 18, 2023, this research does not involve personal information, commercial interests, and will not cause harm to the human body, and can be exempted from ethical review.

## Differentially Expressed Gene (DEG) Identification

The DEGs between the septic shock and normal groups were analyzed using the "limma"R Package (version 3.48.1) and the results were visualized using heatmaps and volcano plots. Differential expression was considered statistically significant based on the $Log_2FC > 1$ and adjusted $P < 0.05$ criteria.

## Gene Set Enrichment Analysis (GSEA)

Epigenetic differences between biological states were examined through GSEA. The GSEA[16] software (http://software.broadinstitute.org/gsea/index.jsp) was used to examine the comprehensive relationship between lung infection-induced septic shock and autophagy-related genes (ARGs), with the $P < 0.05$ and $NES > 1.0$ criteria indicating statistical significance.

## Weighted Gene Co-Expression Network Analysis (WGCNA)

The distribution of outcome-related genes is often delineated using WGCNA.[17] Herein, data from the GSE33118 dataset were analyzed using the "WGCNA" R package (version 1.72–1), with the soft thresholding (0–1) approach employed to divide the data into modules and identify those most relevant to septic shock. Each module had a Module Eigengene (ME) and a distinct color.

## Differentially Expressed Autophagy-Related Gene (DEARG) Identification

According to research, lung injury could disrupt the autophagy levels in immune cells, strongly influencing patient prognosis.[18] Herein, 1167 ARGs were extracted from pertinent databases,[19–21] and the Venn diagram was used to overlay DEGs, ARGs, and the "MEroyalblue" module (defined as DEARGs).

## Enrichment Analyses

Gene Ontology (GO)[22] analysis is commonly employed for the comprehensive functional characterization of genes and primarily encompasses Biological Processes (BPs), Molecular Functions (MFs), and Cellular Components (CC). On the other hand, to reveal associations between genes and pathways, the Kyoto Encyclopedia of Genes and Genomes (KEGG)[23] is often used. Herein, GO and KEGG enrichment analyses were performed using the "clusterProfiler" R package (version 4.9.3). The results were visualized using Sangerbox 3.0[24] and those with the $P < 0.05$ criteria indicating statistical significance.

## Protein-Protein Interaction (PPI) Networks

The STRING database[25] was used to construct the PPI network, which was visualized using Cytoscape software (version 3.10.1).[26] Using the MCC algorithm-based Cytohubba plugin Screening Centre Gene, incorporated into the Cytoscape platform, the DEARGs in each PPI network were assigned values and subsequently sorted, with the ten most highly connected genes identified as the hub genes.

## Receiver Operating Characteristic (ROC) Curve Analysis

Using the GSE33118 and GSE131761 datasets, we constructed ROC curves and assessed the diagnostic power of central genes using MedCalc statistical software (https://www.medcalc.org). Area Under the Curve (AUC) values ≥ 0.8 indicated optimal diagnostic efficacy.

## In Vivo Experimental Protocols

C57BL/6 mice (6W; 20–22g) from Beijing Viton Lihua Technology were used for in vivo experiments. All mice received standard chow and were kept in an experimental environment that conformed to National Institutes of Health standards.[27] The Ethics Committee of the First Affiliated Hospital of Nanchang University reviewed and approved all animal-related experimental procedures (Approval number: CDYFY-IACUC-202310QR004). All the laboratory procedures were followed the "Laboratory Animals-Guideline of welfare and ethics" of the State Standard of P.R. China for the welfare of animals (GB/T 35892-20181).

The animals were categorized into three experimental groups (n = 6/group). The sham group underwent open surgery without Cecal Ligation and Puncture (CLP) one week after commencing standardized feeding. In the CLP group, the animals were fasted for 12 h before modelling, and then anaesthetized via intraperitoneal injection of 1.5% pentobarbital sodium. Following that, the abdominal hair was removed using a hair removal cream before sterilizing the bare skin with 75% alcohol. Subsequently, the tissues between the skin and the abdominal cavity were sequentially incised to expose the blind end of the cecum. Subsequently, the upper 1/3 of the blind end of the cecum is ligated. A 21G needle was then used to pass through the ligated intestinal tubes. Finally, the cecum was returned to its original position after the intestinal contents were extruded. The peritoneum and skin were then closed sequentially with 4–0 silk sutures. In the CLP + Rapamycin (Rapa) group, one week before performing the CLP procedure, the mice were administered Rapa via intraperitoneal injection at a dose of 2 mg/kg every two days.

## Hematoxylin and Eosin (H&E) Staining

After euthanasia induction, the animal's lung tissues were harvested. Subsequently, the tissues fixed in a 10% paraformaldehyde solution. They were then paraffin-embedded and cut into 5-μm thick sections for analysis. Subsequently, the sections were subjected to H&E staining using the Servicebio kit (Cat# G1005) following the manufacturer's instructions.

## Cell Transfection

First, the si-WIPI1 (Antisense: UGUUGUGGAUAUAGAUGGA), si-NLRC4 (Antisense: UAGUCAUCAAACUCCCAGC), and si-NC lentiviral vectors (Beijing Tsingke Biotech Co., Ltd., China) were transfected into MH-S cells. Following the manufacturer's instructions, lipoMAX (ThermoFisher, USA) was then employed

for transfection at a concentration of 50 μM. The efficacy of the process was quantified through real-time fluorescence quantitative Polymerase Chain Reaction (qPCR).

## Cell Culture and Treatment

First, MH-S cells (Cell Bank of the Chinese Academy of Sciences) were inoculated into the RPMI-1640 medium supplemented with 10% Fetal Bovine Serum (FBS) and 1% penicillin-streptomycin, and then routinely cultured in an incubator at 37°C and 5% $CO_2$ per standard laboratory practice.

To understand the role of autophagy dysregulation in sepsis-induced lung injury and the capacity of autophagy-related genes to regulate lung injury, we categorized the MH-S cells into five groups: Control (Con), LPS, LPS + Rapa, LPS + si-WIPI1, and LPS + si-NLRC4. In the Con group, MH-S cells were only cultured for 48 h following standard protocols. In the LPS group, the cells were cultured for 36 h under standard conditions and then stimulated with 100 ng/mL LPS (L5293, Sigma-Aldrich, USA) for 12 h. In the LPS +Rapa group, the cells were subjected to a 24-h pre-treatment with Rapa (HY-10219, MedChemExpress, USA) and then stimulated with 100 ng/mL LPS. In the LPS + si-WIPI1 group, the cells were transfected with si-WIPI1 for 36 h and then stimulated with 100 ng/mL LPS for 12 h. In the LPS + si-NLRC4 group, the cells were transfected with si-NLRC4 for 36 h and then stimulated with 100 ng/mL LPS for an additional 12 h.

## Cell Counting Kit-8 (CCK-8) Assay

Cellular viability was assessed using the CCK-8 assay kit (C0037, Beyotime, China) following the manufacturer's instructions. The cell survival rate was determined as a percentage of the control.

## Apoptosis Assay

Apoptosis rates were analyzed through flow cytometry (Agilent, NovoCyte D3000, excitation wavelength of 488 nm and emission wavelength of 578 nm) using an apoptosis detection kit (BB-4101, BestBio, China). After subjecting the cells in each group to the aforementioned treatments, they were collected via centrifugation at 300×g for 5 min at 4°C. Add 10 μL Annexin V-FITC (20 min) and 5 μL PI (5 min), both incubated in the dark at 4°C. The sum of the early and late apoptosis rates represented the overall apoptosis rate.

## Lysosome Assay

The Lyso-Tracker Red (C1046, Beyotime, China) staining assay was performed to evaluate the degree of autophagy. The pre-processed cells from each group were stained with 0.1% Lyso-Tracker Red for 30 minutes at room temperature in the dark. They were the analyzed using a Fluorescence microscope (Zeiss, Germany) to measure the fluorescence intensity, which reflected the levels of autophagy of the cells.

## Western Blot Assay

Pre-treated MH-S cells were lysed with the RIPA lysate (P0013C, Beyotime, China) to extract total proteins. The concentration of total protein was quantified by the Bradford Kit (P0006C, Beyotime, China) method. Subsequently, the protein samples were mixed with 1x loading buffer and boiled at 100 °C for 8 min. 25 μg of the protein was subjected to 8–12% SDS-PAGE and transferred to a 0.22 μm PVDF (Millipore, Sigma, USA) membrane. The membrane was blocked with 5% skimmed milk powder for one hour at room temperature, and then incubated with the primary antibodies at 4 °C overnight. It was then washed three times with TBST, and incubated for 1h with a secondary antibody (1:10000, SA00001-1, SA00001-2, Proteintech, China) at room temperature. The proteins bands were then visualized using the enhanced chemiluminescence (ECL, US EVERBRIGHT, S600) reagents and analyzed with Bio-Rad's Image Lab software. The quantitative analysis and statistical evaluation of protein bands were conducted using the ImageJ software (version 1.8.0; NIH). β-actin was selected as the internal control.

## qPCR

Total RNA samples were extracted from the pre-treated cells and lung tissues using commercially available RNA extraction kits (ER501-01, TransGen, China). Synthesis of cDNA using the SevenClever cDNA Synthesis Kit (SM136,

SEVEN, China). The qPCR SuperMix (AQ132-11, TransGen, China) and the CFX Connect system were employed to perform qPCR reactions. Briefly, 20 μL of cDNA reaction solution was mixed and pre-denatured at 94°C for 30 sec, thermal cycling at 94°C for 5 sec, and denaturation at 60°C for 30 sec, for a total of 40 cycles. β-actin served as the internal control. The relative mRNA expression of target genes was calculated using the the $2^{-\Delta\Delta CT}$ method.[28] Details of the gene used in this research are shown in Supplementary Table 1.

## Immune Cell Infiltration Analysis

The proportion of infiltrating immune cells was determined using the "CIBERSORT" R package (version 1.07, http://CIBERSORT.stanford.edu/). The gene expression data were normalized in the GSE33118 followed by determination of the proportion of 22 immune cells with the CIBERSORT algorithm. The results were visualized using the Sangerbox platform (http://vip.sangerbox.com).

## Single-Cell Sequencing Analysis

Single-cell sequencing data for critical DEARG were derived from the single-cell portal (https://singlecell.broadinstitute.org/single_cell). Single-cell sequencing data for normal healthy human blood specimens and septic adult blood specimens were derived from SCP43,[29] SCP548[30] and SCP2155.[31]

## Statistical Analysis

Statistical analyses were performed using R (version 4.2.2; Dotmatics) and GraphPad Prism 9 (version 9.0.2) software. All results were expressed as mean ± SD. Comparisons between less than three groups were performed using unpaired two-tailed Student's *t*-test, while comparisons between more than three groups were performed using one-way ANOVA. Results or differences with the $P < 0.05$ criteria indicating statistical significance.

# Results

## Overall Research Protocol

Figure 1 shows this study's flowchart. First, DEARGs in the GSE33118 dataset were identified followed by a series of scoring screenings to obtain the hub genes. Second, in vivo and in vitro experiments were conducted to validate the altered autophagy characteristics and identify the key genes. Third, the immune relevance and single-cell distribution of the key genes were explored.

## Autophagy Correlated With Changes in the Sepsis Transcriptome

GSEA, a commonly employed method for evaluating the genetic association between a transcriptome and disease phenotype,[32,33] was used to assess the mechanisms of autophagy in sepsis. According to the results, ARGs correlated with the clinical phenotype of sepsis (NES = 1.357; P = 0.003) (Figure 2A), suggesting that ARGs dysregulation is essential for characterizing the sepsis transcriptome sequencing data and that sepsis correlated with autophagy disorders.

## DEG Identification

Based on the GSE33118 dataset, two groups were created: Healthy and sepsis. A subsequent bioinformatic comparison yielded 1518 DEGs (Supplementary Table 2), of which 754 and 764 were downregulated and upregulated, respectively. The DEGs in the sepsis group were visualized using heatmaps (Figure 2B) and volcano plots (Figure 2C).

## Wgcna

WGCNA, a powerful tool for clustering genes with similar expression patterns commonly employed in gene association analysis, was used to analyze the identified genes.[34,35] First, clustering analysis was performed using the "fashcluster" approach (Figure 2D). Second, an automated network and detection module was constructed, based on $\beta = 7$ and $R^2 = 9$ (Figure 2E). Third, comparable modules within the cluster were identified and merged, and comparable modules within the merged cluster were identified (Figure 2F). Ultimately, 14 distinct gene modules were identified, each comprising

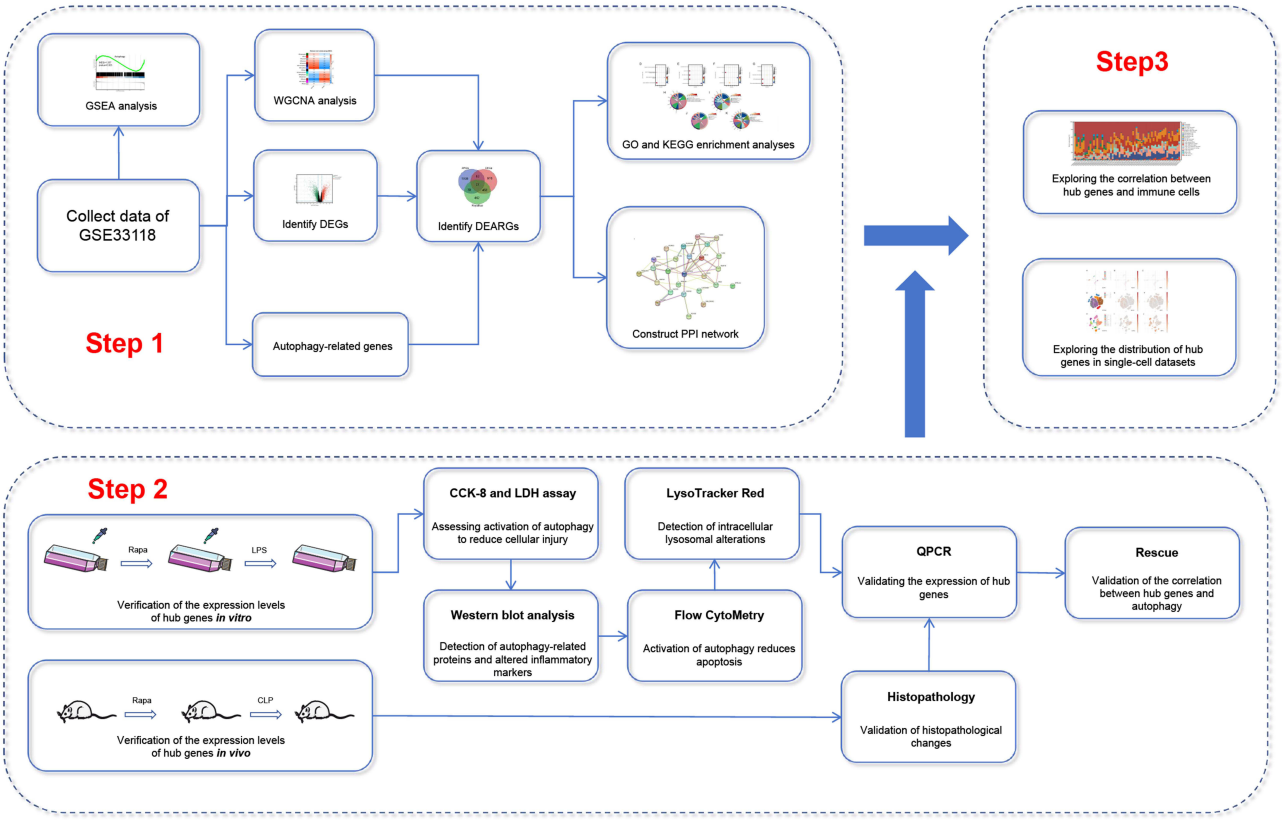


**Figure 1** The flow chart for this study.
**Abbreviations**: GSEA, gene set enrichment analysis; WGCNA, weighted gene co-expression network analysis; GEO, Gene Expression Omnibus; DEGs, differentially expressed genes; ARG, autophagy-related gene; DEARG, differentially expressed ARG; PPI, protein-protein interaction; GO, Gene Ontology; KEGG, Kyoto Encyclopedia of Genes and Genomes; CCK-8, Cell Counting Kit-8; qPCR, Quantitative Real-time Polymerase Chain Reaction.

a comparable set of genes (Figure 2G). According to the module-trait analysis results, multiple modules exhibited a correlation with sepsis, with the MEroyalblue module, comprising 978 genes, correlating most prominently and positively with sepsis (correlation = 0.9; $P < 1e^{-200}$, Figure 2H).

## DEARG Identification

A total of 1,518 DEGs, 978 MEroyalblue module-related genes and 1,167 ARGs (Supplementary Box 1) were identified and subsequently overlapped (Figure 3A) to obtain 27 common genes (DEARGs, Supplementary Box 2). Subsequent investigation was conducted into the distribution (Figure 3B) and genetic correlation (Figure 3C) of the DEARGs in sepsis. The findings suggested that the identified DEARGs may be crucially involved in sepsis pathogenesis via autophagy modulation.

## GO and KEGG Enrichment Analyses

To investigate the relationship between DEARGs and SALI, we elucidated the DEARGs-associated functions and pathways. Regarding BPs, DEARGs were primarily involved in cellular responses to external stimuli, positive macrophage regulation, negative regulation of leukocyte apoptotic processes, and vesicle organization regulation (Figure 3D). Regarding MFs, DEARGs were primarily involved in phosphatidylinositol binding, phospholipid binding, and caspase binding (Figure 3E). In CCs, DEARGs were mainly involved in vesicular membranes, autophagosomes, and autophagosome membranes (Figure 3F). On the other hand, the KEGG enrichment analysis revealed that DEARGs were mainly involved in Toll-Like Receptor (TLR) signaling pathways, Shigella, and autophagy (Figure 3G). Furthermore, the cross-talk mapping of genes and pathways revealed associations between genes and different functions or pathways, suggesting that the roles of DEARGs in sepsis are complex (Figure 3H–K).

## Hub Gene Identification

Given the complex interplay of multiple functions and pathways among the identified DEARGs, we constructed a PPI network to further elucidate the underlying mechanisms (Figure 4A). The DEARG network diagram was then visualized using Cytoscape software to identify the hub genes and functional modules within the earlier identified DEARGs (Figure 4B). Notably, the key modules overlapped completely with the hub genes (Figure 4C), including MAPK14, NLRC4, FADD, VIM, TLR5, IRS2, BIRC5, EEF2, WIPI1, and WDFY3 (Figure 4D). Figure 4E illustrates the fold difference of these hub genes in sepsis, along with their corresponding p-values.

## Internal and External Validation

After the hub genes were identified, we further explored the diagnostic properties of the hub genes for septic lung injury. AUC were determined by constructing separate ROC curves for hub genes derived from the GSE33118 and GSE131761 datasets. In the GSE33118 dataset, the expression of hub genes was compared between sepsis patients and healthy

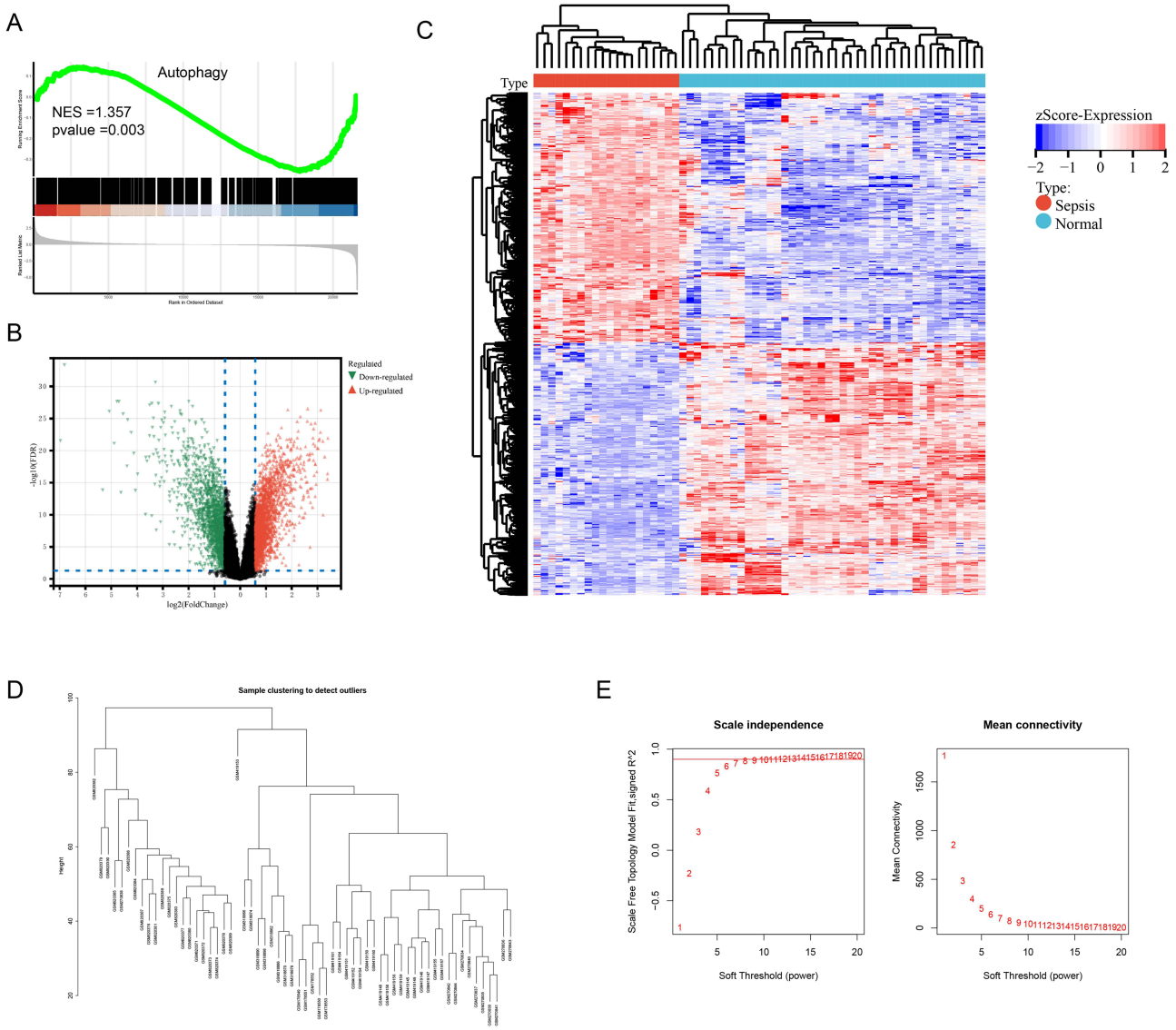


**Figure 2** Continued.


https://doi.org/10.2147/JIR.S510691

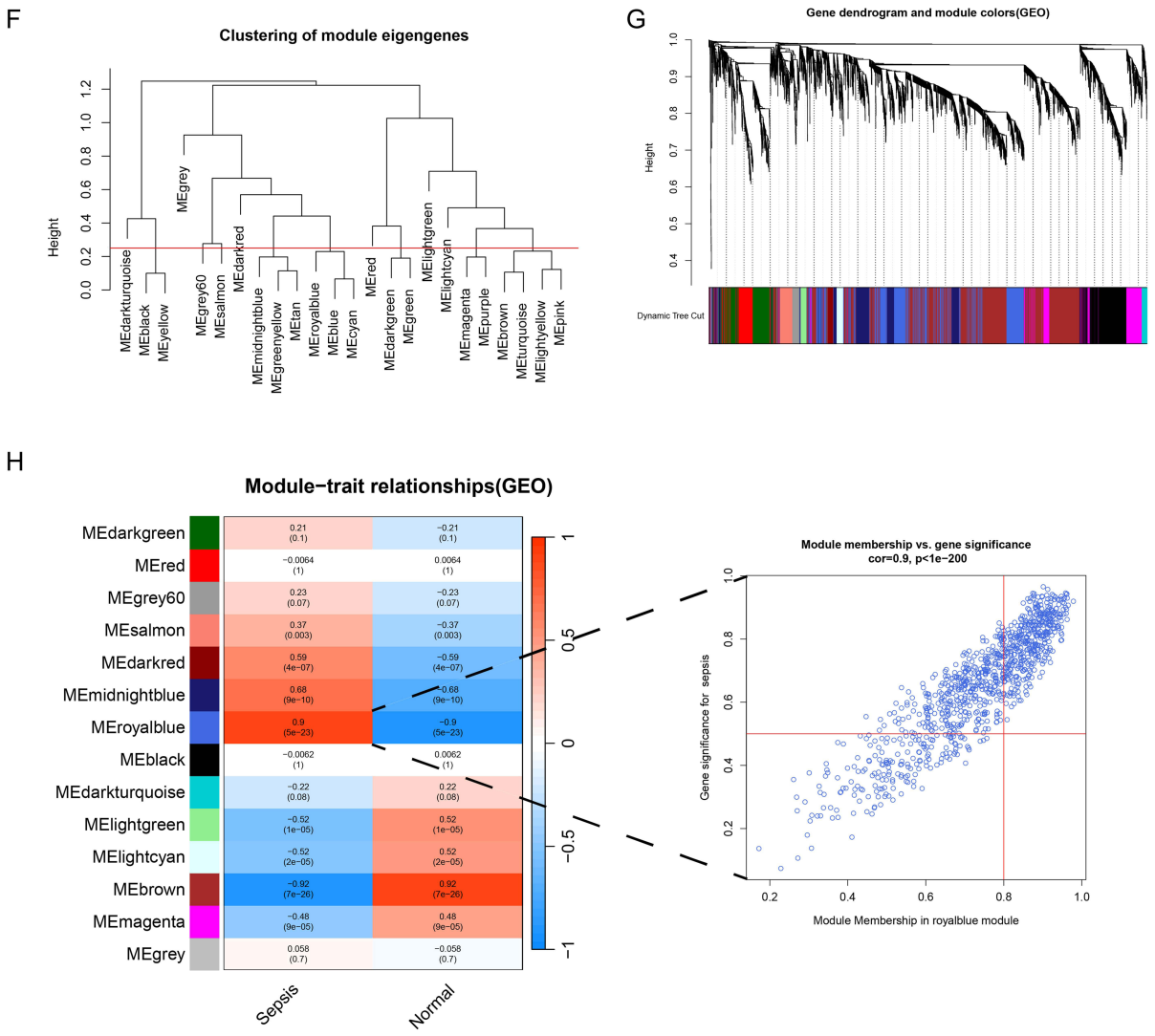


**Figure 2** Gene set-related phenotypes and the identification of differentially expressed genes. (**A**) GSEA of GSE33118. (**B**) Volcano plot of DEGs in GSE33118. The green dots represent low expression and the red dots represent high expression. (**C**) Heatmap clustering of genes with markedly different expression in Sepsis compared with normal samples. The blue squares represent genes with low expression, red squares represent genes with high expression ($log_2FC > 1$ and adjusted $P < 0.05$). Subsequently, GSE33118 was analysed by WGCNA. (**D**) Sample clustering dendrogram based on Euclidean distance to detect outliers. (**E**) Network topology analysis under several soft-threshold powers. (**F**) Clustering of module eigengenes with the threshold set at 0.25 to merge the modules that were comparable in the cluster tree. (**G**) Clustering dendrogram of genes with different similarities based on topological overlap and the assigned module color. (**H**) Different modules were produced, shown in different colors by aggregating genes with strong correlations into the same module. Relevance of members in the MEroyalblue module and sepsis. GSEA, gene set enrichment analysis; DEGs, differentially expressed genes; WGCNA, weighted gene co-expression network analysis; cor, correlation.

controls (Figure 4F). The average AUC of all hub genes was > 0.8, indicating that they correlated with sepsis (Figure 4G). The GSE131761 dataset was used for external validation, wherein the expression of key genes between the two groups was also validated (Figure 4H). The AUC of IRS2 was < 0.8, whereas that of the remaining hub genes was > 0.9 (Figure 4I), suggesting the former's poor diagnostic ability. The remaining nine hub genes showed an excellent diagnostic capability, further suggesting a potential correlation between autophagy and sepsis.

## In vitro Validation

To explore the relationship between autophagy and SALI. We developed an LPS-induced cell injury model using MH-S cells.[36] We then detected changes in autophagy features and hub genes' expression levels in the model. Initially, alterations in LC3 and P62, commonly used autophagy biomarkers,[37] were assessed at the protein level. After treating

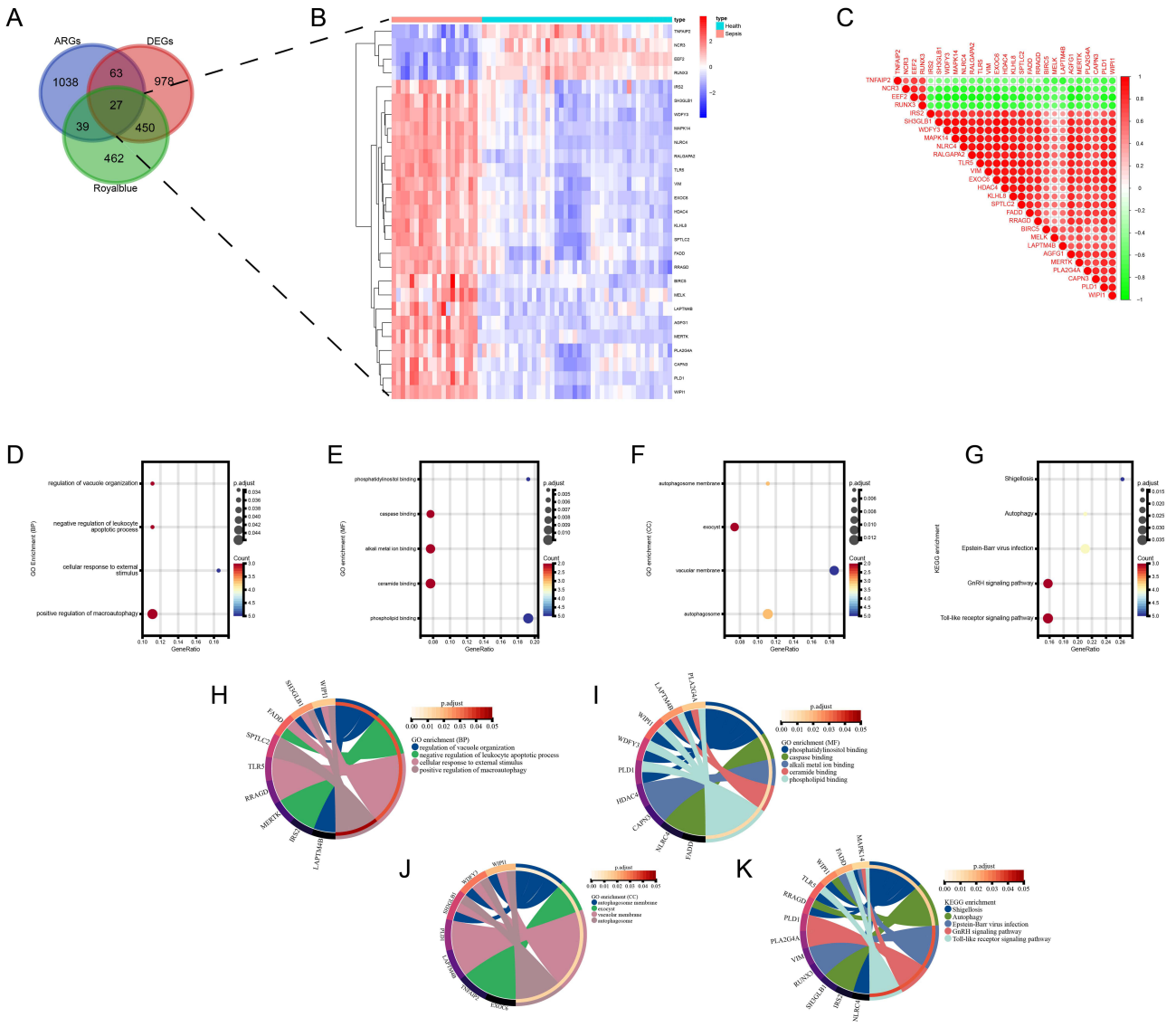


**Figure 3** GO and KEGG enrichment analyses were conducted on the DEARGs from the GSE33118. (**A**) Venn diagram (https://bioinformatics.psb.ugent.be/webtools/Venn/) showing gene overlap between the genes of the MEroyalblue module, DEG and ARG. (**B**) Heatmap of overlapping gene expression between the healthy and sepsis groups. (**C**) Correlation analysis between overlapping genes. Overlapping genes were subjected to GO and KEGG enrichment analyses; GO analyses included three analysis pathways: BP (**D**), MF (**E**) and CC (**F**); KEGG analyses focused on pathway analyses (**G**). And we visualised the crosstalk between overlapping genes and pathways in BP (**H**), MF (**I**), CC (**J**), KEGG (**K**) using dot line plots. GO, Gene Ontology; KEGG, Kyoto Encyclopedia of Genes and Genomes; DEGs, differentially expressed genes; ARG, autophagy-related gene; BP, biological processes; MF, Molecular Function; CC, Cellular Component.

MH-S cells with LPS, the LC3 II/I ratio was reduced and P62 protein expression was elevated, whereas Rapa-pretreated cells reversed these changes (Figure 5A and B). We further evaluated the protein levels of IL-6 and NLRP3, which could reflect the degree of inflammation during sepsis.[2] As anticipated, Rapa administration resulted in lower IL-6 and NLRP3 protein expressions compared to the LPS group. Similarly, LPS-stimulated intracellular lysosomal levels in MH-S cells were significantly reduced. However, Rapa reversed the lysosomal reduction caused by LPS (Figure 5C). Subsequent experiments were conducted to detect the apoptosis rates. According to the results, Rapa pretreatment reversed LPS-induced apoptosis in MH-s cells (Figure 5D and E). Additionally, the cell viability assay revealed that LPS decreased cell viability, a phenomenon that Rapa also reversed (Figure 5F). We further examined the IL-6 mRNA expression, and found that Rapa downregulated IL-6 mRNA expression, suggesting that autophagy activation could reduce lung inflammation (Figure 5G). These findings collectively imply that autophagy induction during sepsis could protect against adverse effects.


https://doi.org/10.2147/JIR.S510691

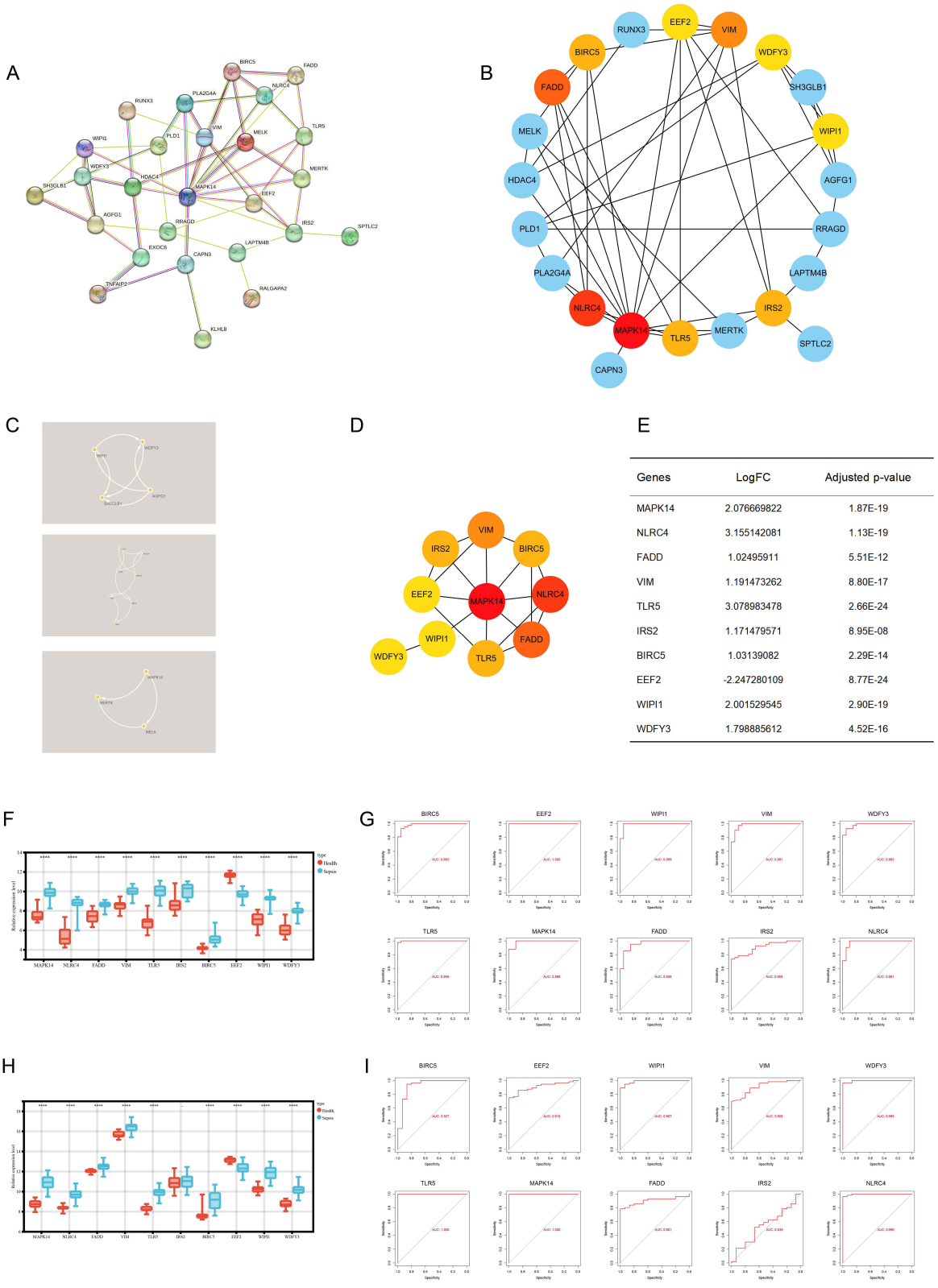


| Genes | LogFC | Adjusted p-value |
|---|---|---|
| MAPK14 | 2.076669822 | 1.87E-19 |
| NLRC4 | 3.155142081 | 1.13E-19 |
| FADD | 1.02495911 | 5.51E-12 |
| VIM | 1.191473262 | 8.80E-17 |
| TLR5 | 3.078983478 | 2.66E-24 |
| IRS2 | 1.171479571 | 8.95E-08 |
| BIRC5 | 1.03139082 | 2.29E-14 |
| EEF2 | -2.247280109 | 8.77E-24 |
| WIPI1 | 2.001529545 | 2.90E-19 |
| WDFY3 | 1.798885612 | 4.52E-16 |

**Figure 4** Identification of hub genes and modules, and diagnostic capabilities. (**A**) The construction of PPI networks for DEARGs via the STRING database. Hub genes (**B**) and key Modules (**C**) were identified by the MCODE plugin using the K-means clustering algorithm (degree cutoff =2, node score cutoff =0.2, K-core =2). (**D**) Crosstalk between 10 hub genes by MCC algorithm. (**E**) $Log_2FC$ and adjusted p-values of the 10 hub genes in GSE33118. (**F**) The relative expression of hub genes in GSE33118. (**G**) ROC curves show the diagnostic capability of hub genes in GSE33118. (**H**) The relative expression of hub genes in GSE131761. (**I**) ROC curves show the diagnostic capability of hub genes in GSE131761. *$p$ < 0.05, **$p$ < 0.01, ***$p$ < 0.005, ****$p$ < 0.001, ns = not significant. Data are presented as the mean ± SD, n ≥ 3. PPI, protein–protein interaction; DEARGs, differentially expressed of autophagy-related genes; ROC, Receiver Operating Characteristic.

Subsequently, the hub genes were subjected to qPCR analysis, revealing that NLRC4 and WIPI1 were upregulated in the LPS group compared to the control group. In contrast, Rapa reduced the expression of NLRC4 and WIPI1 (Figure 5H–P). These findings suggest a potential association of NLRC4 and WIPI1 with autophagy dysregulation in SALI.

## In vivo Validation

In order to ensure the reliability of the experimental results, an in vivo model was developed for the purpose of validation. First, the mice were pretreated with Rapa (2mg/kg for 2 days, 1W). Lung tissues were then collected after 24 h of CLP modelling. The HE staining results showed structural damage to the alveolar structures, increased inflammatory cell infiltration, and alveolar septa thickening (Figure 6A), with the CLP group exhibiting the highest pathology scores (Figure 6B). Regarding the degree of tissue inflammation, the CLP group exhibited a persistently elevated IL6 expression, whereas the Rapa-pretreated group showed no notable increase (Figure 6C). Subsequently, the NLRC4 and WIPI1 gene expression levels were examined. Consistent with the cellular level examination results, the CLP group showed elevated NLRC4 and WIPI1 gene expression levels. Notably, Rapa treatment suppressed the expression of these genes (Figure 6D and E).

## Silencing NLRC4 and WIPI1 Expression Suppressed Alveolar Macrophage Inflammatory Responses Through Autophagy

To silence the expression of NLRC4 and WIPI1 and verify the effect of transfection, si-RNAs targeting the two genes were transfected into MH-S cells (Figure 6F and H). To further establish whether NLRC4 and WIPI1 played a role in autophagy regulation, protein changes in LC3 II/I and P62 were detected based on the earlier stated groupings (Figure 6G and I). According to the results, the LPS-stimulated si-NLRC4 group exhibited up-regulation of LC3 II/I ratio and down-regulation of P62 protein expression. Additionally, NLRP3 protein levels were downregulated following si-NLRC4 treatment. Similarly, the LPS-stimulated si-WIPI1 group exhibited up-regulation of LC3 II/I ratio and down-regulation of P62 protein expression. Additionally, NLRP3 protein levels were downregulated following si-WIPI1 treatment. Furthermore, the IF results revealed that silencing NLRC4 and WIPI1 attenuated LPS-induced lysosomal downregulation (Figure 6J). Cell viability assays further showed that NLRC4 and WIPI1 downregulation resulted in higher cell viability compared to the LPS group (Figure 6K). Additionally, apoptosis detection experiments revealed that NLRC4 and WIPI1 downregulation could mitigate the LPS-induced apoptotic damage (Figure 6L and M). The above results suggest that NLRC4 and WIPI1 may regulate SALI via autophagy.

## Relationship Between NLRC4, WIPI1, and Immune Cells

As SALI is associated with dysregulation of the immune cell environment,[5] we further explored the relationship between NLRC4 and WIPI1 and immune cells. Herein, the proportion of infiltrating immune cells in the GSE33118 dataset was examined (Figure 7A), revealing significant differences in neutrophils, macrophages, T cells, B cells, and mast cells between septic patients and the control group (Figure 7B). These cells were designated as Differentially Infiltrating Immune Cells (DIICs), and correlations among them were visualized using a heatmap (Figure 7C). Notably, the key genes (NLRC4, WIPI1) correlated significantly with DIICs (Figure 7D and E). In other words, NLRC4 and WIPI1 correlated significantly with immune cells such as macrophages, neutrophils, T cells, and B cells (Supplementary Figure 1). These findings suggest that the identified DEARGs not only participated in macrophage autophagy regulation but might have also modulated immune cell infiltration in sepsis.

## Single-Cell Distribution of NLRC4 and WIPI1 in Human Blood Specimens

To assess the distribution of key genes (NLRC4, WIPI1) in human blood, their expression was examined in single-cell sequencing data using the Single Cell Portal (SCP). Although the key DEARGs were predominantly expressed in monocytes (Figure 8A–C), they were also found in other cell types, including B cells and Dendritic Cells (DCs) (Figure 8D–F). Further single-cell data analyses revealed that WIPI1 was predominantly present in type II pneumocytes,

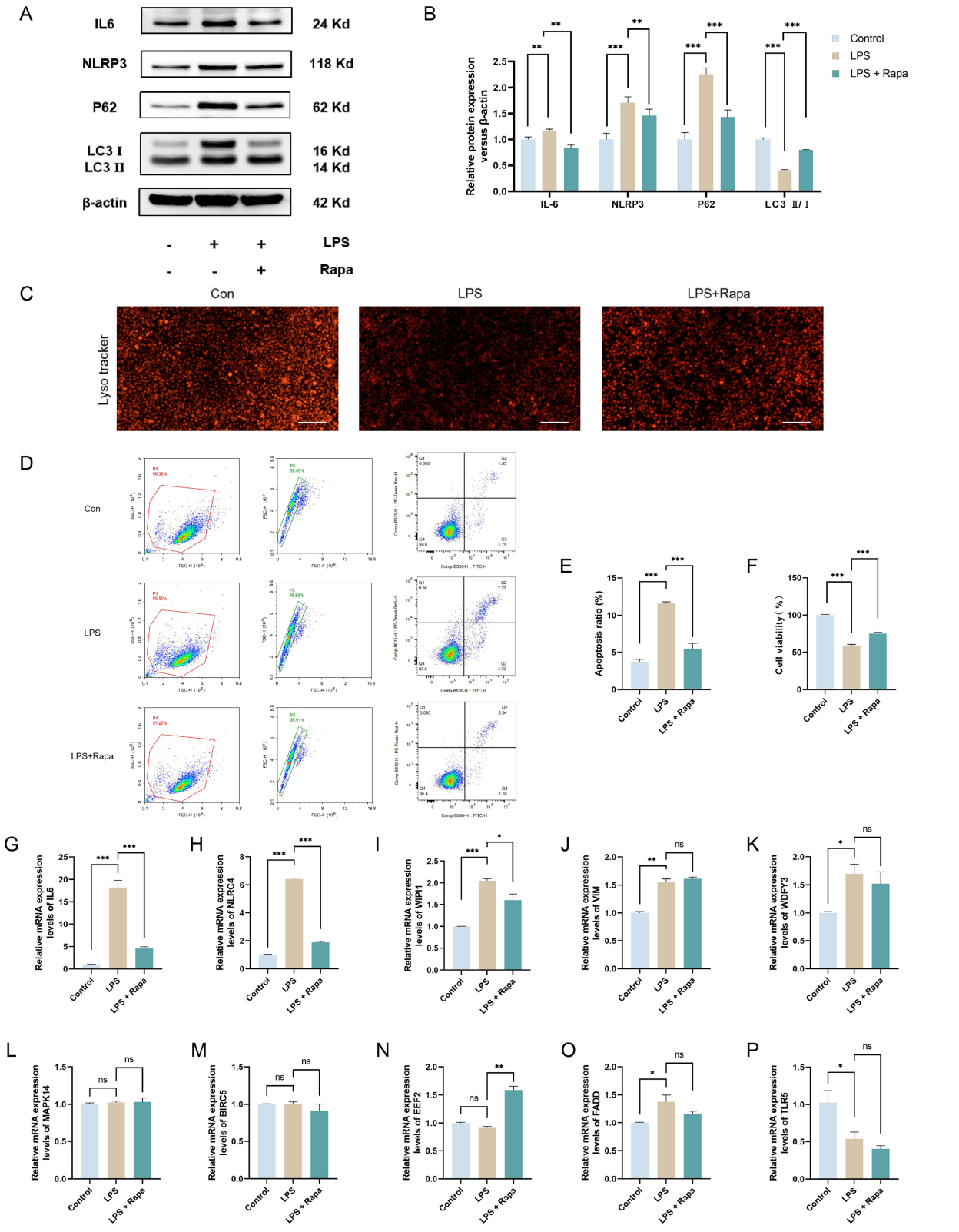


**Figure 5** Detecting autophagy features and assessing hub gene expression in vitro. (**A**) Western blotting to detect the expression of autophagy-related proteins (LC3B, P62) as well as inflammation-related proteins (NLRP3, IL6). (**B**) Relative expression of proteins (LC3B, P62, NLRP3, IL6). (**C**) Detection of intracellular lysosome number by fluorescence microscopy. (**D**) Detection of apoptosis by flow cytometry. (**E**) Apoptosis rate of cells in each group (early apoptosis + late apoptosis). (**F**) The viability of the cells was determined through the utilisation of the CCK-8. The mRNA expression levels of IL6 (**G**), NLRC4 (**H**), WIPI1 (**I**), VIM (**J**), WDFY3 (**K**), MAPK14 (**L**), BIRC5 (**M**), EEF2 (**N**), FADD (**O**), and TLR5 (**P**) in all groups of cells after treatments. *$p < 0.05$, **$p < 0.01$, ***$p < 0.005$, ns = not significant. Data are presented as the mean ± SD, n ≥ 3. CCK-8, Cell Counting Kit-8.

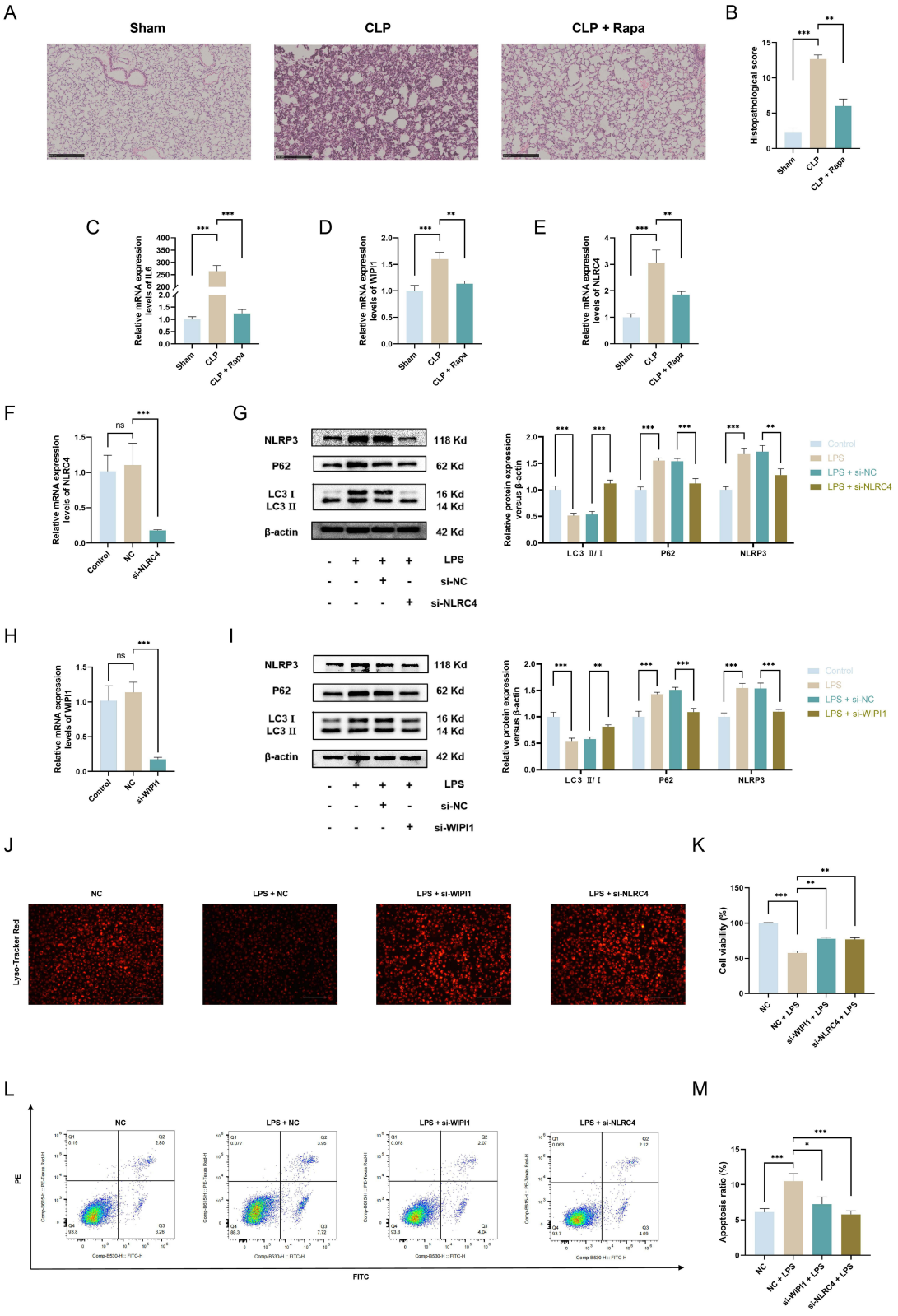


**Figure 6** Key gene (NLRC4 and WIPI1) detection in in vivo and rescue experiments for key genes. (**A**) Pictures of pathological sections (HE) of lungs from mice treated with CLP. (**B**) Pathological section scoring. mRNA expression levels of IL6 (**C**), WIPI1 (**D**), and NLRC4 (**E**) in mouse lung tissue. (**F**) Validation of transfection efficiency of si-NLRC4. (**G**) Detection of related proteins (LC3B, P62, NLRP3) in MH-S cells stimulated by silencing NLRC4. (**H**) Validation of transfection efficiency of si-WIPI1. (**I**) Detection of related proteins (LC3B, P62, NLRP3) in MH-S cells stimulated by silencing WIPI1. (**J**) Changes of lysosomal fluorescence after silencing of NLRC4 or WIPI1. (**K**) Cell viability assay after silencing of NLRC4 or WIPI1. (**L**) Proportion of apoptotic cells after silencing NLRC4 or WIPI1 detected by flow cytometry. (**M**) Apoptosis rate of cells in each group. *$p < 0.05$, **$p < 0.01$, ***$p < 0.005$, ns = not significant. Data are presented as the mean ± SD, n ≥ 3.


https://doi.org/10.2147/JIR.S510691

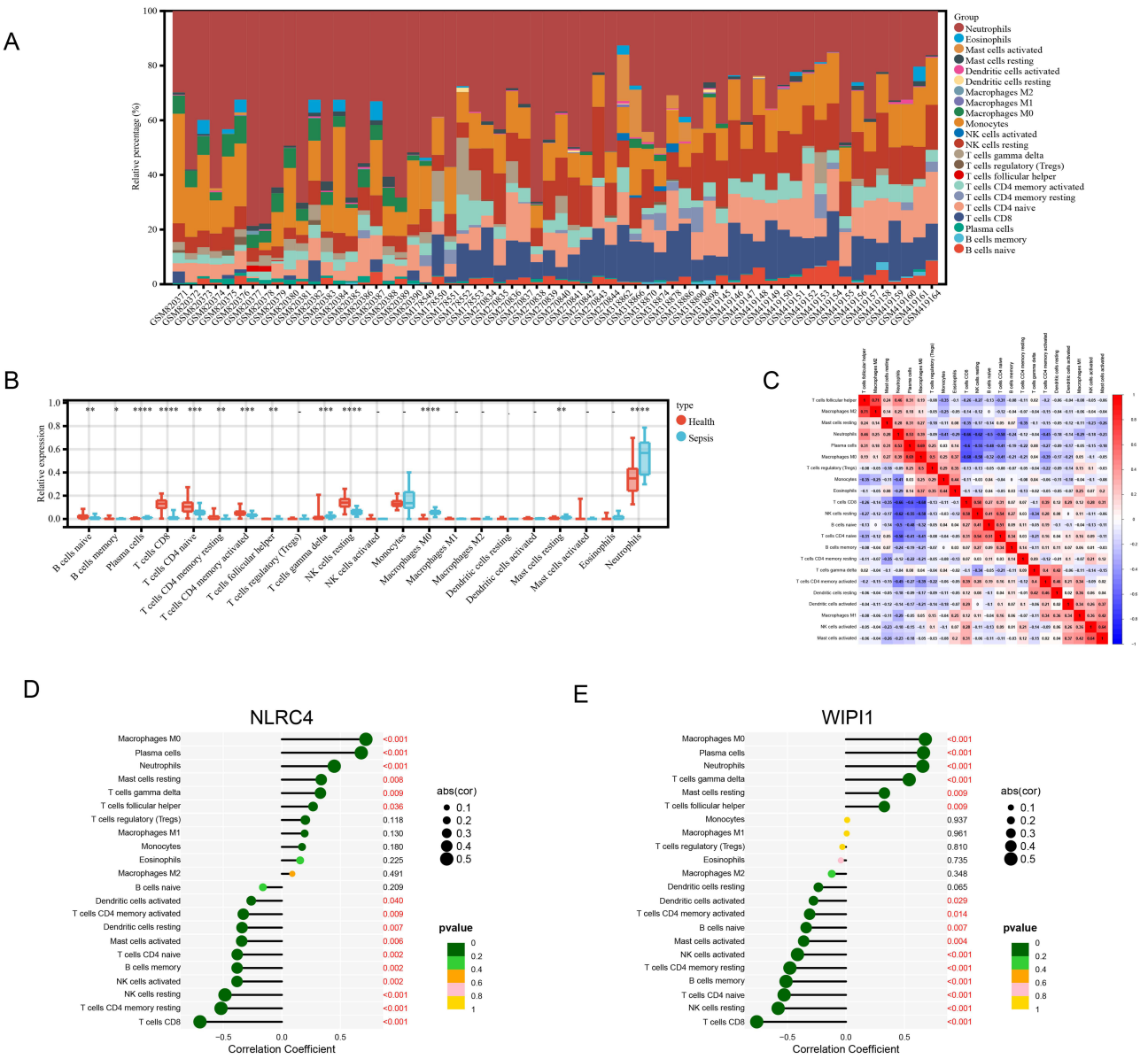


**Figure 7** Immune infiltration analysis of GSE33118, and correlation analysis of key genes with immune cells. (**A**) The proportion of infiltrating immune cells in normal and sepsis samples from GSE33118. (**B**) Differential analysis of infiltrating immune cells in normal and sepsis samples from GSE33118. (**C**) Correlation analysis between infiltrating immune cells in GSE33118. (**D**) correlation between NLRC4 and DIICs. (**E**) correlation between WIPI1 and DIICs. DIICs: differentially infiltrating immune cells. *$p$ < 0.05, **$p$ < 0.01, ***$p$ < 0.005, ****$p$ < 0.001, ns = not significant. Data are presented as the mean ± SD, n ≥ 3.

type I pneumocytes, and epithelial cells in lung injury samples, whereas NLRC4 was mostly present in the mitotic cell cycle and myeloid cells (Figure 8G–I). This finding further supports the hypothesis that both NLRC4 and WIPI1 correlated with immune cells.

## Discussion

Septic Acute Lung Injury (SALI) represents a serious threat not only to patients' lives, but also to their quality of life around the world.[4] SALI is characterised by intricate physiological mechanisms, which renders it challenging to identify effective molecular targets for intervention.[5] Recent studies have demonstrated that the activation of mitochondrial autophagy has the potential to attenuate lung injury.[38] Herein, we explored the role of autophagy in the pathophysiological processes of sepsis.

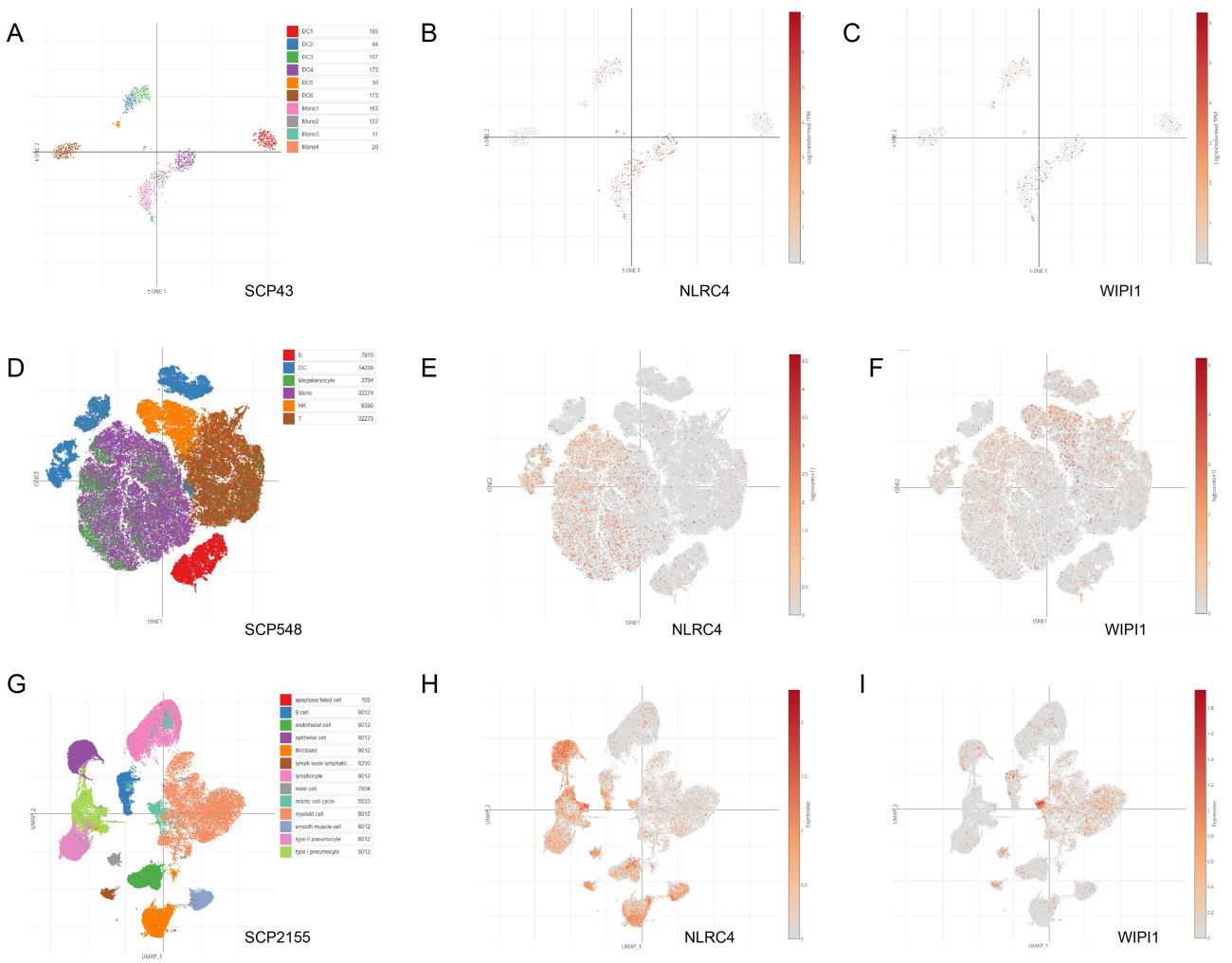


**Figure 8** Analysis of the distribution of key genes in single cells. (**A**) Distribution of different cell types in SCP43. Single-cell distribution of NLRC4 (**B**) and WIPI1 (**C**) in SCP43. (**D**) Distribution of different cell types in SCP548. Single-cell distribution of NLRC4 (**E**) and WIPI1 (**F**) in SCP548. (**G**) Distribution of different cell types in SCP2155. Single-cell distribution of NLRC4 (**H**) and WIPI1 (**I**) in SCP2155.

Specifically, in vitro and in vivo studies confirmed that LPS stimulation inhibiting autophagy, activating inflammatory vesicles, and increasing apoptosis rates and inflammatory factor levels. At the same time, Rapa could restore autophagy levels and reduce inflammation in MH-S cells. Furthermore, the flow cytometry results revealed that agonized autophagy could reduce apoptosis. We also found that only NLRC4 and WIPI1 were upregulated in the LPS-stimulated group and that Rapa could modulate their expression levels. Notably, MAPK14, the gene with the most pronounced difference, according to bioinformatics analysis results, was not significantly different in the in vitro experiments. There could be two explanations for this phenomenon. First, there may not be significant differences in its gene expression levels because MAPK14's functional role in sepsis development is mainly dependent on its phosphorylation.[39] Second, our in vitro validation model was the septic lung injury model and other sepsis injury models may exhibit differential MAPK14 expression at the gene level.

Our subsequent analyses revealed a significant correlation between immune cells (macrophages, neutrophils, T cells, and B cells) and the two key genes—NLRC4 and WIPI1. Therefore, we hypothesized that autophagy may regulate the abundance of these four immune cells in sepsis. Wang et al[40] reported that the mammalian Target of Rapamycin (mTOR) pathway can regulate autophagy dysfunction in sepsis, leading to $CD4^{+}$T cell apoptosis and subsequent adaptive immune function impairment. Additionally, in sepsis, enhanced autophagy could inhibit macrophage inflammatory vesicle activation and reduce inflammation.[41] Furthermore, TLR stimulation can induce autophagy in B cells, thus reducing


https://doi.org/10.2147/JIR.S510691

their capacity to extract and present fixed antigens.[42] Moreover, in a controlled clinical trial, the blood of septic patients with a good prognosis exhibited enhanced neutrophil autophagy levels, whereas those with a poor prognosis exhibited dysregulated neutrophil autophagy.[43] These research insights suggest the crucial involvement of autophagy in immune cells, as well as in the survival outcomes of sepsis patients, aligning with our research findings which indicated that NLRC4 and WIPI1 correlated significantly with autophagy levels in immune cells, considerably influencing patient prognosis.

Notably, NLRC4, a crucial component of the inflammasome family first identified in 2001 as a pyroptosis-inducing protein, could activate caspase enzymes through its CARD structural domain.[44,45] Furthermore, NLRC4 could play novel roles in complexes with NLR Family Apoptosis Inhibitory Proteins (NAIPs), including phagosome maturation, inducible nitric oxide synthase activation, autophagy regulation, inflammatory mediator secretion, antibody production, T-cell activation, and cell activation, among others.[46] These phenomena align with our findings which revealed that NLRC4 promotes inflammatory niche activation under inflammatory conditions. We also found that autophagy activation can downregulate NLRC4, thus diminishing inflammation. Conversely, NLRC4 downregulation could also enhance autophagy. These findings suggest a potential negative correlation between NLRC4 expression and autophagy in septic lung injury and an NLRC4-autophagic pathways crosstalk.

Moreover, WIPI proteins (WIPI1, WIPI2, WIPI3, and WIPI4) are integral to the autophagic process, serving as phosphatidylinositol effectors within the PROPPIN family of mammalian proteins.[47] Although WIPI1's roles in septic lung injury are yet to be reported in relevant studies, a recent study found that it may mitigate Acute Myocardial Infarction (AMI) progression via autophagy pathway activation.[48] This phenomenon is inconsistent with our findings; hence, we hypothesized a potential association with noncanonical autophagic flux. Another study on Heart Failure (HF) corroborated our hypothesis that selective WIPI1 silencing could inhibit atypical autophagy without affecting the classical autophagy pathway. Additionally, WIPI1 upregulation induced mitochondrial superoxide accumulation, impairing mitochondrial function.[48,49] These findings suggest the need for additional research on the specific molecular functions of WIPI1 in septic lung injury.

This study comprehensively analyzed the potential role of autophagy-related genes (NLRC4 and WIPI1) in sepsis diagnosis, biological functions, and immune cell characteristics, with the results validated both in vitro and in vivo. However, there were some limitations. First, due to the small sample size of the sequencing data and the lack of diverse clinical samples, this may affect the generalizability of the results. Second, the dataset we analyzed lacked detailed clinical data to deeply explore the key genes' association with patient prognosis. Third, the NLRC4 and WIPI1 validation tests were restricted to animal and cellular samples, with crucial human samples lacking. Finally, the specific molecular mechanisms of NLRC4 and WIPI1 were inadequately explored, necessitating additional research.

## Conclusion

Our in vivo and in vitro findings revealed that SALI correlated strongly with autophagy dysregulation, with NLRC4 and WIPI1 attenuating it via autophagy regulation, highlighting their significance as potential therapeutic targets for SALI.

## Data Sharing Statement

The data for this study are available in the material of the article as well as in the figure For more detailed data you can contact the corresponding author.

## Ethics Approval and Consent to Participate

All animal-related experimental procedures were reviewed and approved by the Ethics Committee of the First Affiliated Hospital of Nanchang University (CDYFY-IACUC-202310QR004).

## Acknowledgments

The authors would like to express their gratitude to GSE3311, GSE131761, SCP43, SCP548, and SCP2155 for making their data available for sharing. Thanks to Dr. Shitao Zhao for his help in the bioinformatics section.

## Author Contributions

All authors made a significant contribution to the work reported, whether that is in the conception, study design, execution, acquisition of data, analysis and interpretation, or in all these areas; took part in drafting, revising or critically reviewing the article; gave final approval of the version to be published; have agreed on the journal to which the article has been submitted; and agree to be accountable for all aspects of the work.

## Funding

This research was made possible thanks to the generous support of the National Natural Science Foundation of China (81671894), the Natural Science Foundation of Jiangxi Province (20232ACB206046), and the Jiangxi Province Double Thousand Talent Plan (jxsq2023201040).

## Disclosure

All authors of this study have no conflict of interest.

## References

1. Singer M, Deutschman CS, Seymour CW. et al. The Third International Consensus Definitions for Sepsis and Septic Shock (Sepsis-3). *JAMA*. 2016;315(8):801–810. doi:10.1001/jama.2016.0287
2. Cui Y, Yang Y, Tao W, et al. Neutrophil Extracellular Traps Induce Alveolar Macrophage Pyroptosis by Regulating NLRP3 Deubiquitination, Aggravating the Development of Septic Lung Injury. *J Inflamm Res*. 2023;16:861–877. doi:10.2147/jir.S366436
3. Rudd KE, Johnson SC, Agesa KM, et al. Global, regional, and national sepsis incidence and mortality, 1990-2017: analysis for the Global Burden of Disease Study. *Lancet*. 2020;395(10219):200–211. doi:10.1016/s0140-6736(19)32989-7
4. Lelubre C, Vincent JL. Mechanisms and treatment of organ failure in sepsis. *Nat Rev Nephrol*. 2018;14(7):417–427. doi:10.1038/s41581-018-0005-7
5. Evans L, Rhodes A, Alhazzani W, et al. Surviving sepsis campaign: international guidelines for management of sepsis and septic shock 2021. *Intensive Care Med*. 2021;47(11):1181–1247. doi:10.1007/s00134-021-06506-y
6. Mizushima N, Levine B. Autophagy in mammalian development and differentiation. *Nat Cell Biol*. 2010;12(9):823–830. doi:10.1038/ncb0910-823
7. Kubli DA, Gustafsson AB. Cardiomyocyte health: adapting to metabolic changes through autophagy. *Trends Endocrinol Metab*. 2014;25(3):156–164. doi:10.1016/j.tem.2013.11.004
8. Nishida K, Yamaguchi O, Otsu K. Crosstalk between autophagy and apoptosis in heart disease. *Circ Res*. 2008;103(4):343–351. doi:10.1161/circresaha.108.175448
9. Peng W, Peng F, Lou Y, et al. Autophagy alleviates mitochondrial DAMP-induced acute lung injury by inhibiting NLRP3 inflammasome. *Life Sci*. 2021;265:118833. doi:10.1016/j.lfs.2020.118833
10. Sun Y, Yao X, Zhang QJ, et al. Beclin-1-Dependent Autophagy Protects the Heart During Sepsis. *Circulation*. 2018;138(20):2247–2262. doi:10.1161/circulationaha.117.032821
11. Liu Q, Wu J, Zhang X, et al. Circulating mitochondrial DNA-triggered autophagy dysfunction via STING underlies sepsis-related acute lung injury. *Cell Death Dis*. 2021;12(7):673. doi:10.1038/s41419-021-03961-9
12. Dai W, Zheng P, Luo D, et al. LPIN1 Is a Regulatory Factor Associated With Immune Response and Inflammation in Sepsis. *Front Immunol*. 2022;13:820164. doi:10.3389/fimmu.2022.820164
13. Wynn JL, Cvijanovich NZ, Allen GL, et al. The influence of developmental age on the early transcriptomic response of children with septic shock. *Mol Med*. 2011;17(11–12):1146–1156. doi:10.2119/molmed.2011.00169
14. Barrett T, Wilhite SE, Ledoux P, et al. NCBI GEO: archive for functional genomics data sets--update. *Nucleic Acids Res*. 2013;41(Database issue):D991–D995. doi:10.1093/nar/gks1193
15. Martínez-Paz P, Aragón-Camino M, Gómez-Sánchez E, et al. Distinguishing septic shock from non-septic shock in postsurgical patients using gene expression. *J Infect*. 2021;83(2):147–155. doi:10.1016/j.jinf.2021.05.039
16. Subramanian A, Tamayo P, Mootha VK, et al. Gene set enrichment analysis: a knowledge-based approach for interpreting genome-wide expression profiles. *Proc Natl Acad Sci U S A*. 2005;102(43):15545–15550. doi:10.1073/pnas.0506580102
17. Langfelder P, Horvath S. WGCNA: an R package for weighted correlation network analysis. *BMC Bioinf*. 2008;9(1):559. doi:10.1186/1471-2105-9-559
18. Painter JD, Galle-Treger L, Akbari O. Role of Autophagy in Lung Inflammation. *Front Immunol*. 2020;11:1337. doi:10.3389/fimmu.2020.01337
19. Wang -N-N, Dong J, Zhang L, et al. HAMdb: a database of human autophagy modulators with specific pathway and disease information. *J Cheminform*. 2018;10(1):34. doi:10.1186/s13321-018-0289-4
20. Moussay E, Kaoma T, Baginska J, et al. The acquisition of resistance to TNFα in breast cancer cells is associated with constitutive activation of autophagy as revealed by a transcriptome analysis using a custom microarray. *Autophagy*. 2011;7(7):760–770. doi:10.4161/auto.7.7.15454
21. Homma K, Suzuki K, Sugawara H. The Autophagy Database: an all-inclusive information resource on autophagy that provides nourishment for research. *Nucleic Acids Res*. 2011;39(Database):D986–D990. doi:10.1093/nar/gkq995
22. Gene Ontology Consortium. Gene Ontology Consortium: going forward. *Nucleic Acids Res*. 2015;43(D1):D1049–D1056. doi:10.1093/nar/gku1179
23. Kanehisa M, Goto S. KEGG: kyoto encyclopedia of genes and genomes. *Nucleic Acids Res*. 2000;28(1):27–30. doi:10.1093/nar/28.1.27
24. Shen W, Song Z, Zhong X, et al. Sangerbox: a comprehensive, interaction-friendly clinical bioinformatics analysis platform. *IMeta*. 2022;1(3):e36. doi:10.1002/imt2.36

25. Szklarczyk D, Gable AL, Lyon D, et al. STRING v11: protein-protein association networks with increased coverage, supporting functional discovery in genome-wide experimental datasets. *Nucleic Acids Res*. 2019;47(D1):D607–D613. doi:10.1093/nar/gky1131
26. Shannon P, Markiel A, Ozier O, et al. Cytoscape: a software environment for integrated models of biomolecular interaction networks. *Genome Res*. 2003;13(11):2498–2504. doi:10.1101/gr.1239303
27. Council NR, Earth Do, Studies L, Research IFLA, Care CftUotGft, Animals UoL. *Guide for the Care and Use of Laboratory Animals*. 2010.
28. Livak KJ, Schmittgen TD. Analysis of relative gene expression data using real-time quantitative PCR and the 2(-Delta Delta C(T)) Method. *Methods*. 2001;25(4):402–408. doi:10.1006/meth.2001.1262
29. Villani A-C, Satija R, Reynolds G, et al. Single-cell RNA-seq reveals new types of human blood dendritic cells, monocytes, and progenitors. *Science*. 2017;356(6335):4673. doi:10.1126/science.aah4573
30. Reyes M, Filbin MR, Bhattacharyya RP, et al. An immune-cell signature of bacterial sepsis. *Nat Med*. 2020;26(3):333–340. doi:10.1038/s41591-020-0752-4
31. Fabre T, Barron AMS, Christensen SM, et al. Identification of a broadly fibrogenic macrophage subset induced by type 3 inflammation. *Sci Immunol*. 2023;8(82):eadd8945. doi:10.1126/sciimmunol.add8945
32. Zhang C, Zhang J, Zhang Y, et al. Identifying neutrophil-associated subtypes in ulcerative colitis and confirming neutrophils promote colitis-associated colorectal cancer. *Front Immunol*. 2023;14:1095098. doi:10.3389/fimmu.2023.1095098
33. Wang X, Fu S, Yu J, et al. Renal interferon-inducible protein 16 expression is associated with disease activity and prognosis in lupus nephritis. *Arthritis Res Ther*. 2023;25(1):112. doi:10.1186/s13075-023-03094-8
34. Wang Z, Liu J, Wang Y, et al. Identification of Key Biomarkers Associated with Immunogenic Cell Death and Their Regulatory Mechanisms in Severe Acute Pancreatitis Based on WGCNA and Machine Learning. *Int J mol Sci*. 2023;24(3):3033. doi:10.3390/ijms24033033
35. Gao X-M, Zhou X-H, Jia M-W, Wang X-Z, Liu D. Identification of key genes in sepsis by WGCNA. *Prev Med*. 2023;172:107540. doi:10.1016/j.ypmed.2023.107540
36. Liu F, Peng W, Chen J, et al. Exosomes Derived From Alveolar Epithelial Cells Promote Alveolar Macrophage Activation Mediated by miR-92a-3p in Sepsis-Induced Acute Lung Injury. *Front Cell Infect Microbiol*. 2021;11:646546. doi:10.3389/fcimb.2021.646546
37. Debnath J, Gammoh N, Ryan KM. Autophagy and autophagy-related pathways in cancer. *Nat Rev mol Cell Biol*. 2023;24(8):560–575. doi:10.1038/s41580-023-00585-z
38. Meng R, Sun Z, Chi R, et al. Overexpression of Parkin promotes the protective effect of mitochondrial autophagy on the lung of rats with exertional heatstroke. *J Intensive Med*. 2025;5(1):89–99. doi:10.1016/j.jointm.2024.07.004
39. Zhang X, Chen C, Ling C, et al. EGFR tyrosine kinase activity and Rab GTPases coordinate EGFR trafficking to regulate macrophage activation in sepsis. *Cell Death Dis*. 2022;13(11):934. doi:10.1038/s41419-022-05370-y
40. Wang H, Bai G, Chen J, Han W, Guo R, Cui N. mTOR deletion ameliorates CD4 + T cell apoptosis during sepsis by improving autophagosome-lysosome fusion. *Apoptosis*. 2022;27(5–6):401–408. doi:10.1007/s10495-022-01719-y
41. Liu F, Yang Y, Peng W, et al. Mitophagy-promoting miR-138-5p promoter demethylation inhibits pyroptosis in sepsis-associated acute lung injury. *Inflam Res*. 2023;72(2):329–346. doi:10.1007/s00011-022-01675-y
42. Lagos J, Sagadiev S, Diaz J, et al. Autophagy Induced by Toll-like Receptor Ligands Regulates Antigen Extraction and Presentation by B Cells. *Cells*. 2022;11(23):3883. doi:10.3390/cells11233883
43. Park SY, Shrestha S, Youn YJ, et al. Autophagy Primes Neutrophils for Neutrophil Extracellular Trap Formation during Sepsis. *Am J Respir Crit Care Med*. 2017;196(5):577–589. doi:10.1164/rccm.201603-0596OC
44. Lage SL, Longo C, Branco LM, da Costa TB, Buzzo C, Bortoluci KR. Emerging Concepts about NAIP/NLRC4 Inflammasomes. *Front Immunol*. 2014;5:309. doi:10.3389/fimmu.2014.00309
45. Egan MS, Zhang J, Shin S. Human and mouse NAIP/NLRC4 inflammasome responses to bacterial infection. *Curr Opin Microbiol*. 2023;73:102298. doi:10.1016/j.mib.2023.102298
46. Deretic V. Autophagy as an innate immunity paradigm: expanding the scope and repertoire of pattern recognition receptors. *Curr Opin Immunol*. 2012;24(1):21–31. doi:10.1016/j.coi.2011.10.006
47. Ren J, Liang R, Wang W, Zhang D, Yu L, Feng W. Multi-site-mediated entwining of the linear WIR-motif around WIPI β-propellers for autophagy. *Nat Commun*. 2020;11(1):2702. doi:10.1038/s41467-020-16523-y
48. Liu W, Shen J, Li Y, et al. Pyroptosis inhibition improves the symptom of acute myocardial infarction. *Cell Death Dis*. 2021;12(10):852. doi:10.1038/s41419-021-04143-3
49. Byrnes K, Blessinger S, Bailey NT, Scaife R, Liu G, Khambu B. Therapeutic regulation of autophagy in hepatic metabolism. *Acta Pharm Sin B*. 2022;12(1):33–49. doi:10.1016/j.apsb.2021.07.021